Proceedings of the European Conference "Physics of Magnetism '99", Poznań 1999

$Ce_3Cu_3Sb_4$: A CANTED ANTIFERROMAGNETIC SEMIMETAL

P. WACHTER, L. DEGIORGI, G. WETZEL, H. SCHWER, K. MATTENBERGER

Laboratorium für Festkörperphysik, Eidgenössische Technische Hochschule Zürich
8093 Zürich, Switzerland

T. HERRMANNSDÖRFER AND P. FISCHER

Laboratory for Neutron Scattering, Paul Scherrer Institute PSI
5232 Villigen, Switzerland

It has been claimed by Patil et al., *Solid State Commun.* **99**, 419 (1996) that $Ce_3Cu_3Sb_4$ is the first Ce-based semiconducting ferromagnet. In this paper it is shown, mainly with Hall effect and far infrared spectroscopy that no gap in the excitation spectrum exists, as well above as below the magnetic ordering temperature. A maximum in the resistivity near T_C is due to trapped magnetic polarons. The resistivity is an effect of the mobility of the charge carriers. The structure of the magnetic unit cell has been determined with elastic neutron scattering.

PACS numbers: 75.30.–m, 78.20–e, 72.15.Eb, 72.15.Gd

1. Introduction

Ce-based compounds are always good for a surprise. The Ce mono-chalcogenides and mono-pnictides are well investigated materials [1] and no other class of compounds has evoked so much theoretical interest than the Ce pnictides. Magnetic susceptibilities are dominated by crystal field effects but near 300 K the full effective magnetic moment of $2.54\mu_B$ is achieved. However, the saturation moment of the free ions $gJ = 2.14\mu_B$ is rarely obtained, even in fields of 100 kOe [1]. Crystal field effects may be the reason for this. Famous are the many magnetic phases of CeSb, which is also the material which exhibits the largest Kerr rotation [2]. In many cases hybridization effects and moment quenching of the magnetic moments go in parallel and phenomena of intermediate valence, e.g. in CeN [3] or heavy fermion behavior as e.g. in $CeCu_2Si_2$ [4], which even becomes a superconductor at 0.7 K, are abundant. So-called Kondo insulators like $Ce_3Pt_3Bi_4$ [5] or CeNiSn [6] are materials which seem to have a gap and the Fermi level in the gap, so they behave like semiconductors. Whereas this has been verified by far infrared optical measurements in the case of $Ce_3Pt_3Bi_4$ [7] (a material in which Ce is formally

tetravalent) it has been shown recently that in carefully prepared CeNiSn single crystals the features of a gap disappear [8]. Even in the high T_C superconductor $Nd_{2-x}Ce_xCuO_4$ Ce again plays an anomalous role, inasmuch as this is the first n-type high T_C superconductor [9].

Recently [10, 11] it has been reported that with $Ce_3Cu_3Sb_4$ the first semiconducting ferromagnet based on Ce has been discovered, which certainly adds to the anomalous properties of Ce compounds. Magnetic data suggest that the Curie temperature T_C is near 12 K and a band gap of a semiconductor has been calculated from resistivity data. Using the formula $\rho \propto \exp(E_g/2kT)$ yields $E_g \cong 84$ K or $\cong 7$ meV.

In Ref. [10] the resistivity is rising with decreasing temperature without showing a maximum, but in Ref. [11] by the same group of researchers, a maximum of the resistivity at 19 K is reported. In Ref. [12] a maximum of the resistivity near 4 K is shown. A fit of the rising branch with decreasing temperature with the above formula yields an activation energy of 5.2 meV, but these authors never claim $Ce_3Cu_3Sb_4$ to be a ferromagnetic semiconductor. It is obvious that the quality of the samples determines these differences. But in general it is not legitimate to interpret a material with a maximum in the resistivity to be a semiconductor on the high temperature side and a metal on the low temperature side. The electrical conductivity is still a product of the carrier concentration and the mobility and as long as it is not proven which of the two parameters is changing, the claim of a semiconductor is not convincing. In fact between 300 and 30 K, covering most of the rise of the resistivity towards lower temperature, the Hall effect has been measured [12] and no change in carrier concentration has been observed. The mobility, however, can also be thermally activated, in which case one speaks of a trapped magnetic polaron [13, 14] (and references quoted therein), which becomes liberated below T_C of a ferromagnet.

The Hall effect of a ferromagnet near and below T_C must be analyzed and separated into the normal and anomalous Hall effect and one must look also for other means to detect the essential of a semiconductor, namely the gap. Optical measurements, especially in the far infrared and at low temperatures, supply a simple and critical means to detect a gap. The mobility alone can be measured with photoelectric methods, especially when the intrinsic carrier concentration is small.

The motivation to reinvestigate $Ce_3Cu_3Sb_4$ is based on theoretical assumptions [15] to be discussed below that a small Kondo like electronic gap with the Fermi level in the gap can only exist with an even $f-d$ electron count. This is only the case for Sm and Yb compounds and Tm compounds when they are antiferromagnets, because then the magnetic unit cell is twice the chemical unit cell and the $f-d$ count is even again [16]. In trivalent and ferromagnetic Ce compounds the $f-d$ electron count is odd.

2. Sample preparation and characterization

Polycrystalline, single phase $Ce_3Cu_3Sb_4$ was synthesized under Ar atmosphere by arc melting, followed by an annealing of the sample under vacuum. In

the first step stoichiometric amounts of Ce (99.9%), Cu (99.9%) and Sb (spectroscopic purity) have been molten several times by arc in an Ar atmosphere to ensure homogeneity of the sample. In a series of preliminary experiments, performed with an identical procedure, it was substantiated that 4% of stoichiometric excess of volatile Sb has to be added to the starting material to obtain a stoichiometric content in the final product (as determined by X-ray analysis). Using this Sb excess we could avoid the weight control of the sample to detect the Sb loss after each arc melting process. The reaction chamber was always closed and therefore there was no danger of oxidation of the sample, as occurred in Ref. [10]. X-ray powder diffraction detected no impurities of Sb oxides, however, other phases such as traces of CeSb were indicated.

To obtain single phase $Ce_3Cu_3Sb_4$ an additional step had to be performed where the multi-phase sample was sealed under vacuum into a quartz ampoule and annealed in a resistance oven for three weeks at 820°C. In the final product only a single phase of $Ce_3Cu_3Sb_4$ was resolved by X-ray diffraction. Polycrystalline $Ce_3Cu_3Sb_4$ was measured in transmission on a STOE powder diffractometer using Ge mono-chromated CuK_{α_1} radiation. Data were collected in the range $10° \leq 2\theta \leq 120°$ with a position sensitive detector. The material contained no impurities and could be indexed on the basis of a cubic unit cell with $a = 9.7527(1)$ Å. The reflections of the diffractogram were fitted with the Pearson-VII peak profile with a fixed exponent $e = 2.0$. Structure refinement was done with the Rietfeld method using the PFSR program of the STADI-P software [17].

Crystal data of the $Y_3Au_3Sb_4$ structure model were taken from Dwight [18] and background, profile, and structural parameters were refined. Profile and structural refinements converged at low $R_p = 0.043$, $R_{wp} = 0.056$ and $R(I, hkl) = 0.042$. Figure 1 shows the observed, calculated and difference (obs–calc) diffraction pattern. $Ce_3Cu_3Sb_4$ crystallizes in the space group $I\text{-}43d$ with the $Y_3Au_3Sb_4$ structure type which is related to the Th_3P_4 structure. Ce and Cu atoms are located at the 12a and 12b sites, respectively. Sb was refined to $x = 0.0792(2)$ at the 16c (x, x, x) position. Bond lengths in $Ce_3Cu_3Sb_4$ are Ce–Cu = 2.9861 Å, Ce–Sb = 3.419(2) Å, 3.333(2) Å and Cu–Sb = 2.709(2) Å. The crystal structure in real space is shown in Fig. 2 with its Ce, Cu, and Sb coordination polyhedra. We did not find any indication for a tetragonal distortion as reported by Patil et al. [10]; their published diffraction pattern is the same as in Fig. 1, but it contained additional impurities and a reflection denoted as "312". This reflection is the only hint for a tetragonal distortion, all other reflections can be indexed with a cubic cell. A true tetragonal unit cell of $Ce_3Cu_3Sb_4$ should generate much more reflections due to symmetry reduction, so it is most likely that the only real structure of $Ce_3Cu_3S_4$ is the cubic one presented here.

All the following physical measurements on $Ce_3Cu_3Sb_4$ (with the exception of neutron scattering) have been performed on the very same, about 100 mg piece of material from the center of the ingot, from which a chipped off splinter has been used for the above X-ray analysis. In a follow up paper [19] an elastic neutron diffraction investigation of magnetic Ce ordering has been performed on a 10 g piece of material (the whole ingot) and this lump of material was not as

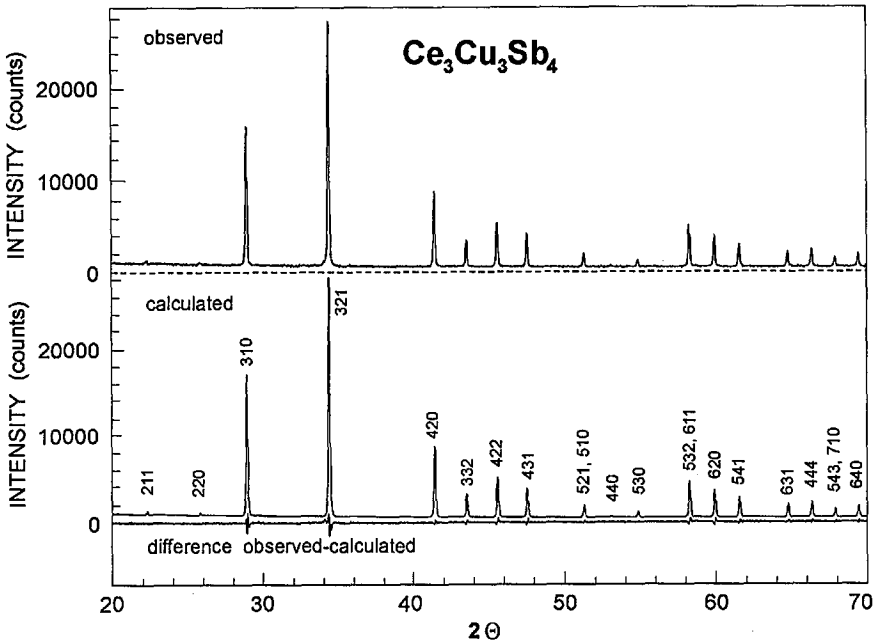

Fig. 1. X-ray powder diffractogram of $Ce_3Cu_3Sb_4$. Top: the observed data; middle: the calculated diffraction pattern, refined with the Rietfeld method; bottom: the difference observed minus calculated.

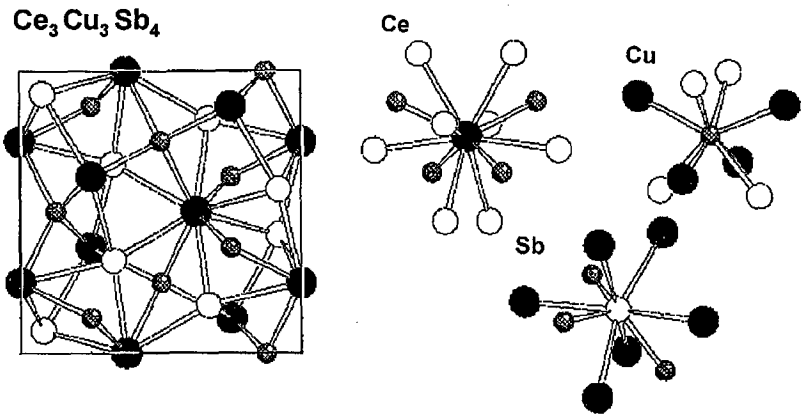

Fig. 2. Crystal structure of $Ce_3Cu_3Sb_4$, with the coordination polyhedra of Ce, Cu, and Sb atoms.

homogeneous as the piece used in the other investigations. In fact it had about 4% of the CeSb phase.

In the course of the growth process of $Ce_3Cu_3Sb_4$ the melting point of this compound has been determined with two different methods. During heating of the sample sealed under vacuum in a molybdenum crucible, both the temperature

change (4°C/min) — measured by pyrometry — and the power increase in an electron beam furnace, heating the crucible (20 W/min), were measured. After a certain time the temperature remained practically constant in spite of further heating. The same temperature was found during a cooling process. Thus this temperature determines the melting point T_m. In a second method the sample was heated inductively in an alumina crucible under 2.5 bar of Ar and observed visually with a pyrometer. With a heating rate of 4°C/min the liquefaction could be easily determined. T_m was found to be 1740±50 K which is much lower than the reported 2295 K [12]. In Ref. [12] the melting points of various $R_3Cu_3Sb_4$ alloys (with R being a rare earth) have been collected and $Ce_3Cu_3Sb_4$ has been claimed to have the highest T_m. Compared with $Gd_3Cu_3Sb_4$ this is improbable since a $4f^1$ material always has a lower T_m than the corresponding, electronically more stable $4f^7$ compound.

3. Magnetic measurements

The inverse of the magnetic susceptibility in a field of 4.67 kOe is shown in Fig. 3 below 70 K. The solid line is a fit with a Curie–Weiss law up to 300 K which yields an effective magnetic moment of $2.59\mu_B$, close to the theoretical value of $2.54\mu_B$. We obtain a paramagnetic Curie temperature θ_p of –3 K. The inset shows the initial susceptibility in a field of 10 Oe. The kink at 12 K indicates the Curie temperature and the plateau at low temperatures is caused by the demagnetizing factor. In Fig. 4 we have plotted the magnetization at 1.5 K in fields up to 100 kOe. It is obvious that there exists a spontaneous magnetization of $2.15\mu_B$ per formula unit or $0.66\mu_B$ per Ce ion. However, even at 100 kOe no saturation is achieved. The saturation moment of Ce^{3+} is $gJ = 2.14\mu_B$ and is missed by a factor 3. Quenched moment systems are common in Ce compounds, but as will be shown below, there is no such gap as exists in a Kondo lattice, a Kondo insulator or a heavy fermion [16] (and references quoted therein). Thus the material is not a simple ferromagnet.

Crystal field effects are small in $Ce_3Cu_3Sb_4$. The low point symmetry S_4 of the Th_3P_4 related structure splits the $J = 5/2$ state into 3 doublets. In analogy with Sm_3S_4 which crystallizes also in the Th_3P_4 structure and has the same $J = 5/2$ ground state we can assume that the Γ_7 is the lowest doublet [20, 21]. Since $Ce_3^{3+}Cu_3^{1+}Sb_4^{3-}$ is electronically the same as CeSb a comparison is permitted. The Ce–Sb separation in the former material is larger than in the fcc CeSb compound but there are 8 Sb anions surrounding each Ce. We then can assume that in large magnetic fields, especially including also the internal Weiss field of a quasi-ferromagnet, magnetic saturation could be achieved, just as is the case for CeSb, where above 50 kOe at 1.5 K the gJ saturation moment of $2.14\mu_B/Ce^{3+}$ is obtained [1]. Experimentally this saturation moment is not reached in $Ce_3Cu_3Sb_4$. Two possibilities can explain the observed behavior: either the alloy is a canted antiferromagnet which yields the spontaneous moment of $0.66/Ce^{3+}$. With increasing field the canting angle is gradually reduced until saturation is achieved. Or the alloy is highly anisotropic, having only in one crystallographic direction the saturation magnetization of $2.14\mu_B$ and in the two others only a weak, linearly increasing magnetization with field.

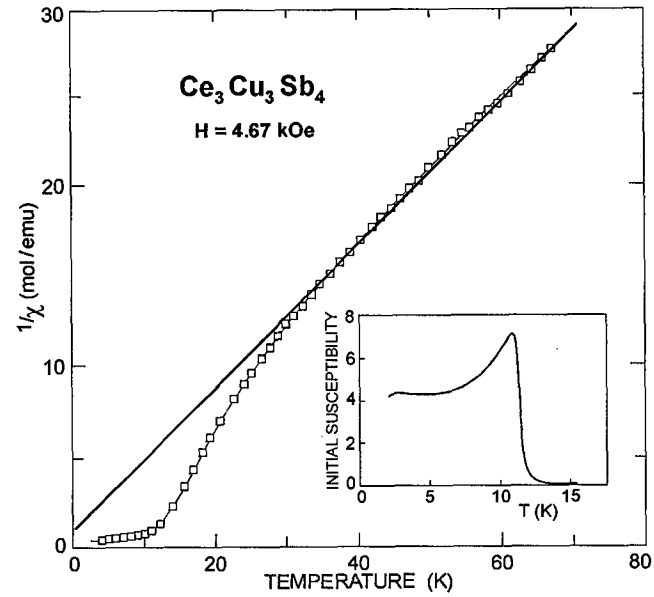

Fig. 3. The inverse magnetic susceptibility of $Ce_3Cu_3Sb_4$ in a field of 4.67 kOe. The inset shows the initial susceptibility in a field of 10 Oe.

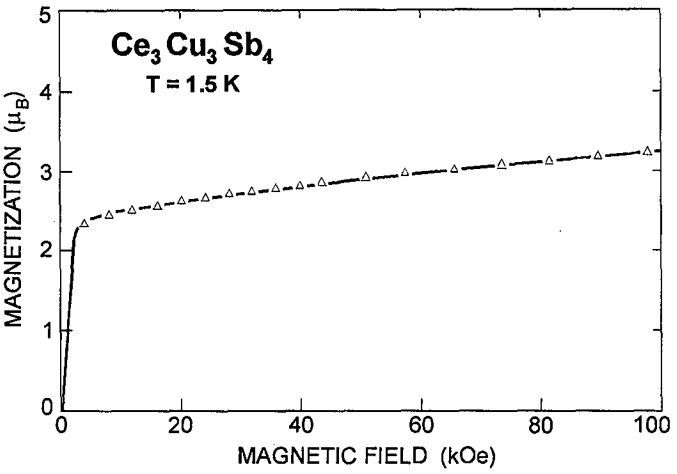

Fig. 4. The magnetization of $Ce_3Cu_3Sb_4$ at 1.5 K.

To decide between these two possibilities an elastic neutron scattering has been performed on the DMC multi detector powder diffractometer situated at a supermirror guide for cold neutrons at SNQ, the Swiss Neutron Source in Villigen [19]. The neutron wavelength $\lambda = 2.556$ Å was obtained from a vertically focusing pyrolytic graphite monochromator, combined with a graphite filter to remove higher order contaminations. Measurements with very good counting statis-

tics (about one day per temperature) were made in the paramagnetic state at 18 K and in the magnetically ordered state at approximately 2 K. Due to the restricted accessible scattering angle range 2θ, absorption corrections were neglected. The neutron pattern shows besides the nuclear diffraction additional antiferromagnetic Bragg peaks as well as ferromagnetic reflections. Based on the space group $I\bar{4}3d$ (No. 220), a group theoretical analysis of the possible "magnetic modes" was performed for the Ce sites (12a) by means of the MODY program. The best agreement between the observed and calculated magnetic neutron intensities was obtained for the irreducible three-dimensional representation τ_5, resulting in the coupling scheme of the magnetic moments summarized in Table. The corresponding canted

TABLE

Canted antiferromagnetic Ce ordering of $Ce_3Cu_3Sb_4$. The I centering (+(1/2,1/2,1/2)) holds. x, y, z denote the positions of the Ce ions in the chemical unit cell, μ_x, μ_y, μ_z = x, y, and z component of the ordered magnetic moment, respectively. $\mu \leq gJ\mu_B$ = magnitude of the magnetic moment per Ce atom.

x	y	z	$\mu_x[\mu_B]$	μ_y	μ_z	μ
0.375	0	0.25	2.1(2)	0.4(1)	0.4(1)	2.1(2)
0.125	0	0.75	2.1(2)	0.4(1)	0.4(1)	2.1(2)
0	0.25	0.375	0.4(1)	0.4(1)	2.1(1)	2.1(2)
0	0.75	0.125	0.4(1)	0.4(1)	2.1(1)	2.1(2)
0.25	0.375	0	0.4(1)	2.1(2)	0.4(1)	2.1(2)
0.75	0.125	0	0.4(1)	2.1(2)	0.4(1)	2.1(2)

antiferromagnetic configuration is illustrated in Fig. 5. It implies shortest Ce–Ce distances of 4.55 Å. The ordered magnetic Ce moment agrees within error limits with the free ion value of Ce^{3+}, i.e. there seems to be in the present case no crystal field or Kondo reduction of the ordered magnetic moment, similar to the case of CeSb [1], as has been suggested already above. From Fig. 3 inset of the initial susceptibility or a direct susceptibility measurement in small fields, it can be seen that magnetic saturation is achieved at low temperatures. For a magnetic single domain crystal of $Ce_3Cu_3Sb_4$ the present model of magnetic ordering yields $1.6\mu_B$ as a resultant ferromagnetic moment component per Ce^{3+} along the direction [111], in fair agreement with $\geq 1.1\mu_B$ to be expected from magnetization measurements for $H \leq 100$ kOe in Fig. 4. In small external magnetic fields presumably magnetic domains are present which favor an average alignment of 1/3 of the magnetic Ce moments along the direction [100]. The increase in the magnetization with the external magnetic field is most probably due to a domain reorientation of net ferromagnetic moments from [100] to [111]. Single crystals would be necessary to confirm this concept.

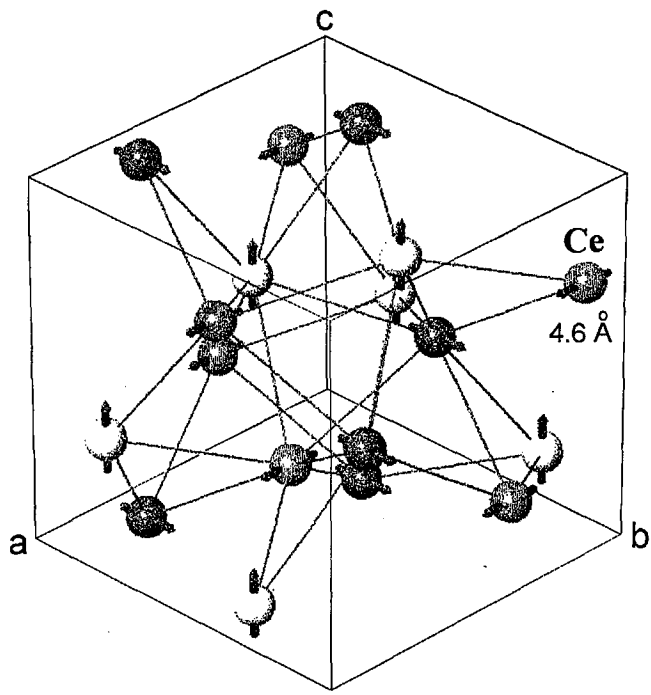

Fig. 5. The magnetic unit cell of $Ce_3Cu_3Sb_4$.

The neutron diffraction measurements in zero external magnetic field clearly show that $Ce_3Cu_3Sb_4$ is not a simple ferromagnet, as claimed by Patil et al. [10]. Instead it is a canted antiferromagnet. The magnetic unit cell is found to be equal to the chemical unit cell.

4. Electrical transport measurements

The electrical resistivity of $Ce_3Cu_3Sb_4$ has been measured as a function of temperature and magnetic field up to 10 T and it is shown in Fig. 6. The resistivity in zero field has a maximum at 17 K and with increasing magnetic field the curve is lowered and the maximum shifts towards higher temperatures. In Ref. [10] no resistance maximum has been observed, but in Ref. [11] a maximum is stated at 19 K. In Ref. [12] a maximum is observed at 4 K. These differences are probably related to the quality of the samples. The rising branch of the resistivity with decreasing temperature has been fitted in all preceding publications with an exponential law $\rho \propto \exp(E_g/2kT)$ and an energy gap of 7 meV [10, 11] and 5.2 meV [12] or 2.3 meV [12], as a result of a confusion in the text and Fig. 4 of Ref. [12], has been obtained. Our fit with an exponential law between 250 and 110 K is shown in the inset of Fig. 6. Using the formula $\rho \propto \exp(E_g/2kT)$ we find E_g to be 5 meV, but we will argue below that one should use rather $\rho \propto \exp(\Delta/kT)$, in which case Δ is 2.5 meV and would correspond to a magnetic binding energy, having nothing to do with Fermi statistics.

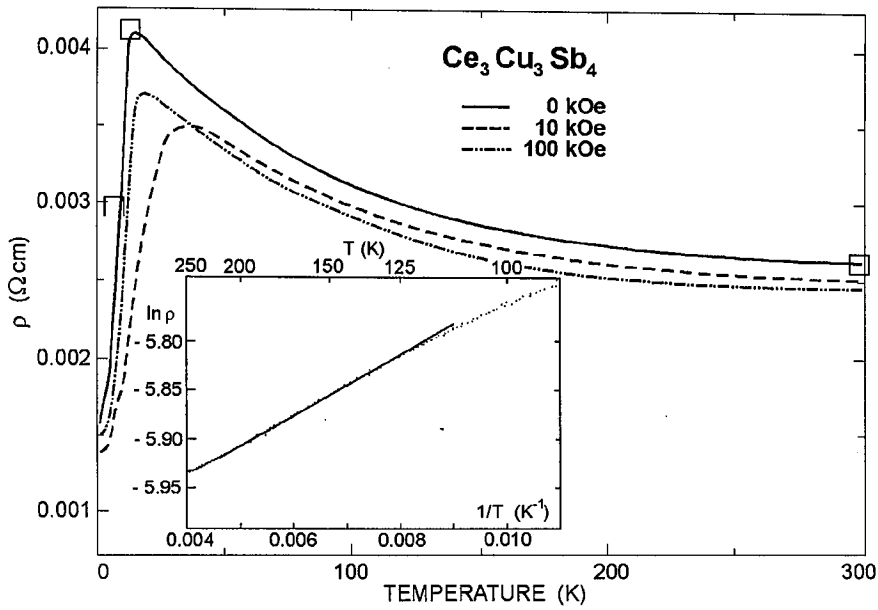

Fig. 6. The resistivity of $Ce_3Cu_3Sb_4$ in zero field, 10 kOe, and 100 kOe. The inset shows a $\ln \rho$ versus $1/T$ plot. The three squares are calculated resistivity values from the optical conductivity given in Fig. 9.

Although for the increasing branch of the resistivity with decreasing temperature a law with an activation energy is found over a certain temperature range, this does not mean that one has a semiconductor which then should change to a metal below T_C [10, 11]. The electrical conductivity is $\sigma = 1/\rho = enb$ with n the carrier concentration and b the mobility and it must at first be established which of the two temperature dependent parameters n or b is dominating the resistivity. For this purpose a Hall effect measurement is necessary.

In Fig. 7 we show the Hall effect of $Ce_3Cu_3Sb_4$ in fields of 10 kOe and 40 kOe between 2 K and 300 K. In Ref. [12] the Hall effect has been measured only down to 30 K, i.e. above the magnetic ordering temperature. The Hall effect changes the sign near 30 K which means one must use a two-band analysis to obtain the carrier concentration. The correct formula for equal scattering processes of electrons and holes would be

$$R_H = -(r/|e|)(b_n^2 n - b_p^2 p)/(|b_n|n + b_p p)^2$$

with $r = \overline{\tau_p^2}/\overline{\tau_p^2}$, the ratio of the relaxation times, $b_{n,p}$ the mobilities and n and p the concentration of the carriers. Even with $r \cong 1$ the number of parameters exceeds the experimental possibilities. Between 50 K and 300 K R_H is positive which means $b_n^2 n < b_p^2 p$ and one has dominantly p conductivity. At about 30 K $R_H = 0$, thus $b_n^2 n = b_p^2 p$. Nothing is known about the band structure of this material but it is reasonable to assume the essential feature is an indirect overlap of the conduction band of Ce^{3+} with a minimum near the Γ point of the Brillouin zone with the p band of Sb^{3-} with a maximum at the Δ point of the Brillouin zone, just as in $La_3Au_3Sb_4$ [22]. The nonmagnetic Cu^{1+} has only empty ($4s$) and

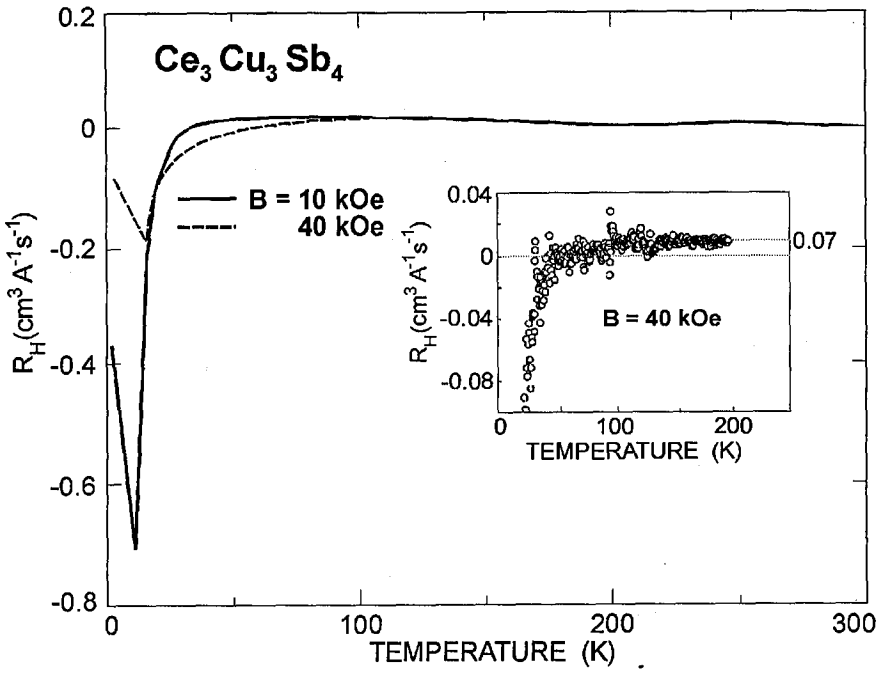

Fig. 7. The Hall effect of $Ce_3Cu_3Sb_4$ in fields of 10 kOe and 40 kOe. The inset shows an enlarged scale at 40 kOe.

full ($3d^{10}$) bands. In this case $n = p$ as in rare earth mono-pnictides [23] and at 30 K $b_n = b_p$ and the material is a self-compensated semimetal.

As seen in Fig. 7, especially in the magnified inset, the Hall effect is positive and temperature independent between 100 K and 300 K, exactly in the temperature range where the resistivity (Fig. 6 inset) shows an activated behavior. Using still the full formula for the Hall effect, but with $r = 1$, and keeping the relation $n = p$, which probably is a condition from the band structure, one can derive a simpler formula for the Hall effect

$$R_H = (1/ep)(b_n - b_p)/(b_n + b_p).$$

Considering that in a two-band model $\sigma = 1/\rho = neb_n + peb_p = pe(b_n + b_p)$, we can derive $\rho = R_H/(b_p - b_n)$ and since R_H is constant and positive between 100 K and 300 K $\rho \propto 1/(b_p - b_n)$, i.e. it depends only on the mobility difference between electrons and holes. If we assume b_p not only larger than b_n (a consequence of a positive resistivity), but much larger $b_p \gg b_n$, then $\rho \propto 1/b_p$. This means that the resistivity increase with decreasing temperature on the high temperature side of the maximum of ρ is only an effect of the mobility which is activated between 110 K and 250 K (Fig. 6, inset).

It has been shown on theoretical grounds [24] that the Hall effect of a two-band model with its many parameters can be replaced by a one-band model, in which case the carrier concentration is the maximum possible. In other words, in the realistic two-band model the carrier concentration is always less than in the

one-band model. In the one-band model $R_H = 1/ep$ and with $R_H = 0.007\ cm^3/(A\ s)$ (Fig. 7 inset) $p = 8.9 \times 10^{20}\ cm^{-3}$, which remains temperature independent between 110 K and 250 K. In the more realistic two-band model p can only be less. Using the lattice parameter of $Ce_3Cu_3Sb_4$ this means that we have a little less than 1 carrier per formula unit, or about 0.3 carriers per Ce^{3+}. The Hall mobility at 250 K is $b_p = 2.8\ cm^2/(V\ s)$, i.e. a very low value. Since the carrier concentration is constant over a large temperature variation this means that the material is not a semiconductor as claimed in Ref. [10].

But the mobility is activated, which means a hopping type mobility, and it is reasonable to assume that the whole temperature dependence of the resistivity as shown in Fig. 6 is due to the mobility. We will show that the whole effect is due to a trapped or a small magnetic polaron. The theory of the magnetic polaron has first been developed by Nagaev [25], but the first experimental evidence of a magnetic polaron has been given by Streit and Wachter [13]. A magnetic polaron is an elementary charge (in this case p) with a spin of 1/2 in a material having ionic magnetic moments as in Ce^{3+}. At temperatures above T_C the spin of the free carrier magnetically polarizes the ion spins in the neighborhood trying to align them parallel to its own spin direction against the temperature induced disorder. In this way the carrier looses energy and becomes magnetically trapped. Its movement is by hopping with an activation energy. Below T_C of a ferromagnet the magnetic exchange interaction between the ion magnetic moments aligns them in parallel, so the carrier gets liberated and the resistivity decreases. At T_C critical spin flip scattering dominates resulting in the maximum of the resistivity. An external magnetic field can help to align the ion spins already above T_C and especially below T_C scattering on different magnetic domains becomes reduced. These effects are surprisingly small in $Ce_3Cu_3Sb_4$ for a claimed ferromagnet. But as we have shown above $Ce_3Cu_3Sb_4$ is not a simple ferromagnet, but a canted antiferromagnet and this is exactly the reason why the magneto-resistance effects are so small. The magnetic polaron finds at all temperatures nonaligned ion spins and can get trapped. In fact this is a further proof of the absence of ferromagnetic order, although a spontaneous magnetic moment exists.

If the activation energy measured in the resistivity is due to the magnetic trapping energy of a small magnetic polaron as argued above we understand that we should not use a formula $\rho \propto \exp(E_g/2kT)$ as for an electronic gap with the Fermi level for $T \to 0$ in the middle of the gap, but $\rho \propto \exp(\Delta/kT)$ with Δ the magnetic binding energy of the small polaron, which then is 2.5 meV.

Below 30 K the Hall effect becomes negative and exhibits a sharp minimum (depending on field) near T_C. The shape of the curve in Fig. 7 is typical for a material having an ordered moment, but the Hall resistivity $\rho_H(B,T) = R_H(B,T)B$, being proportional to R_H, is strongly field dependent near T_C, which is not typical for a simple ferromagnet. The Hall effect must be separated into an ordinary and an extraordinary part. The separation of the Hall resistivity can be made according to the following formula [26]:

$$\rho_H(B,T) = R_o(T)B + 4\pi R_s M(B,T),$$

where R_o is the ordinary Hall effect and R_s the spontaneous Hall effect due to the

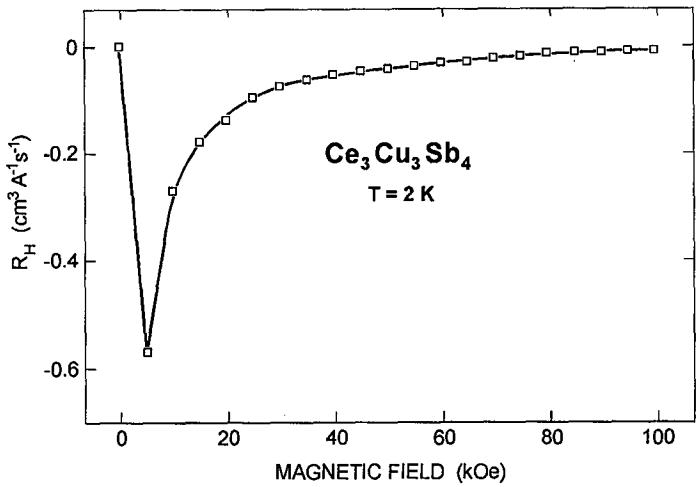

Fig. 8. The field dependence of the Hall effect of $Ce_3Cu_3Sb_4$ at 2 K.

magnetization $M(B,T)$. The formula above can be rewritten as

$$R_H = R_o + 4\pi R_s M/B.$$

In Fig. 8 we show the Hall effect in function of field at 2 K and using Fig. 8 together with Fig. 4 we can make a linear plot of R_H versus M/B from which we can evaluate R_o, the ordinary Hall effect, $R_o = -0.02$ cm^3/(A s) and R_s the spontaneous, extraordinary Hall effect, $R_s = -8\times10^{-3}$ cm^3/(A s). In a single band model analysis, and we recall that this yields the maximum number of carriers, we find $n_o = 3 \times 10^{20}$ cm^{-3} and $n_s = 8 \times 10^{20}$ cm^{-3}. It is obvious that the carrier concentration also at 2 K, i.e. in the magnetically ordered state, is metallic and from the same order of magnitude as at room temperature. It is therefore clear that over the whole temperature range $Ce_3Cu_3Sb_4$ is a metal, in contrast to Refs. [10, 11]. However, the sign of the carriers has changed from positive near room temperature to negative near 2 K. In a two-band model there is no problem with that, especially considering that the condition $n = p$ may no longer be fulfilled at low temperatures where the exchange splitting of the $5d$ band of Ce is certainly not the same as that of the Sb p band. Exactly this has been observed in ferromagnetic variations of TbN and GdN [27].

5. Optical properties

The final decision of a material having a gap of whatever kind is the direct measurement of such a gap. Optical measurements, especially far infrared reflectivity down to the lowest temperatures, have the potential to make a gap visible. Gaps can be in the density of states as in a semiconductor, they can be a Kondo gap or hybridization gap, as in strongly correlated electron systems. The Fermi level can be in the gap or in a density of states peak as in heavy fermions, even gaps of superconductors can be observed optically. Numerous examples exist in the literature (e.g. Refs. [14, 16]).

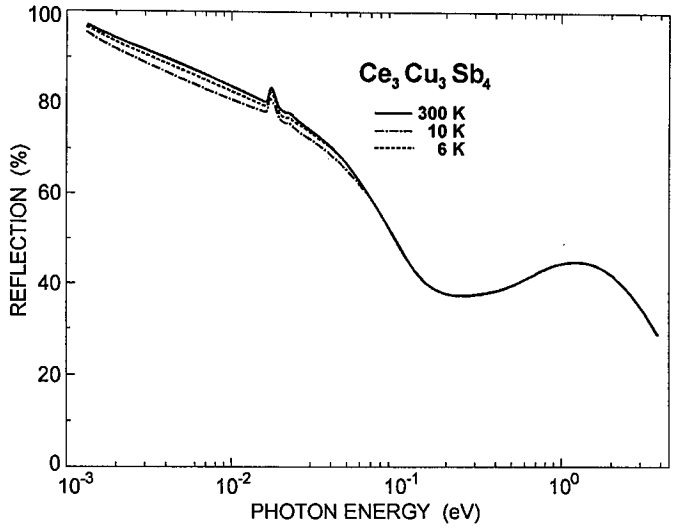

Fig. 9. The optical reflectivity of $Ce_3Cu_3Sb_4$ between 10^{-3} eV and 4 eV photon energy at 6 K, 10 K, and 300 K.

We have measured the optical reflectivity on polished probes of $Ce_3Cu_3Sb_4$ over a photon energy range from 10^{-3} eV to 6 eV between 300 K and 6 K, i.e. above and below T_C. The reflectivity spectrum is displayed in Fig. 9 at 3 different temperatures. The general behavior is that of a metal, with interband transitions peaking near 1 eV and a plasma edge due to free carriers, with a plasma resonance around 0.2 eV. Near 0.02 eV a phonon double peak structure is observable, but the reflectivity is smoothly approaching 100% for $\omega \rightarrow 0$. There is no indication of a gap whatsoever. Below about 0.07 eV the reflectivity exhibits a temperature dependence, inasmuch as the curve near T_C (12 K)is lower than the curve at 6 K. In this photon energy range the damping is mostly determining the shape of the curve, so that we must conclude that at 10 K the damping is stronger than at 6 K or 300 K. The damping is directly related to the electrical resistivity, so that we must expect that the resistivity shows a maximum near T_C. This piece of information corroborates the direct measurement of the resistivity as displayed in Fig. 6. On the other hand, a gap even in the meV range would manifest itself in a clear deviation of the reflectivity from 100% for $\omega \rightarrow 0$. Then, the reflectivity would approach a constant value. Another possibility which cannot be excluded, is a zero gap material as in principle is α Sn. Such a conclusion has been drawn in a similar material, $Ce_3Au_3Sb_4$ [28], but a zero gap material would still be at variance with the statement of a ferromagnetic semiconductor [10, 11].

In Fig. 10 we show the optical conductivity of $Ce_3Cu_3Sb_4$. These results are obtained with a Kramers–Kronig analysis of the reflectivity which yields the real and imaginary parts of the dielectric functions. As extrapolation to $\omega \rightarrow 0$ we use for all three measured temperatures a best fit with the Hagens–Rubens relation (connecting the reflectivity for small ω with the dc conductivity) and as extrapolation towards infinite frequencies we use up to 20 eV a $1/\omega^2$ law and above a

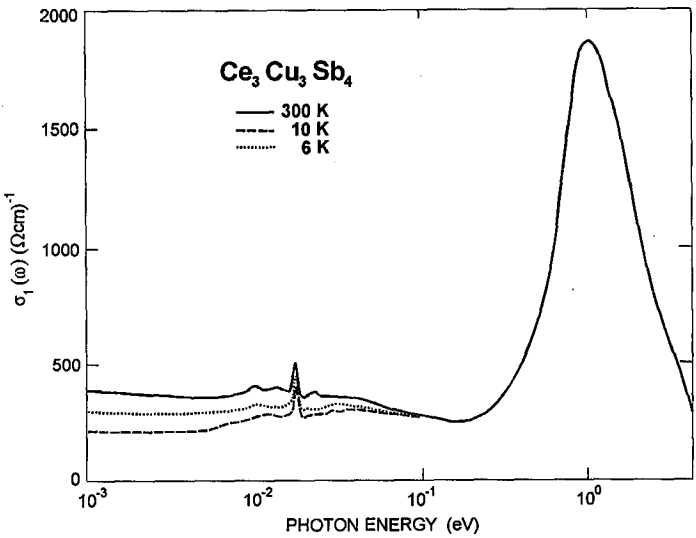

Fig. 10. The real part of the optical conductivity of $Ce_3Cu_3Sb_4$ at 6 K, 10 K, and 300 K.

$1/\omega^4$ power law. The obtained conductivity values of Fig. 10, extrapolated towards $\omega \to 0$, and converted to resistivity values, are indicated in Fig. 6 as squares and they agree surprisingly good with the measured dc resistivity of the same sample. On the other hand, the plasma resonance near 0.2 eV is temperature independent. The plasma resonance $\omega_p^2 = 4\pi ne^2/m^*\epsilon_{opt}$ depends mainly on the carrier concentration, which thus remains temperature independent. This corroborates nicely the Hall effect data.

It can be further seen from Fig. 10 that besides the interband transition near 1 eV and the phonon structure near 0.02 eV a flat broad peak can be discerned also near 0.02 eV, best observed at 10 K. Such a structure can be associated with the signature of magnetic polarons as was first measured for magnetite Fe_3O_4 [29]. In $Ce_3Cu_3Sb_4$ such a peak is nearly one order of magnitude lower in energy than in magnetite (0.25 eV). Nevertheless it scales with the activation energies in the resistivity of both materials.

6. Conclusion

It has been shown above that phase pure and uncontaminated $Ce_3Cu_3Sb_4$ is neither ferromagnetic nor semiconducting, as claimed in Refs. [10, 11]. The material exhibits a spontaneous moment of about 1/3 of the theoretical saturation moment and it cannot be saturated even at 100 kOe. The elastic neutron scattering has revealed that it is a canted antiferromagnet. The carrier concentration is high, corresponding to about 1/3 carrier per Ce^{3+} ion, it is temperature independent in the paramagnetic temperature range, but also in the magnetically ordered state it remains of the same magnitude. The resistivity is dominated by mobility effects and a small (self-trapped or bound) magnetic polaron with a hopping type of mobility explains the transport behavior. The small magneto-resistivity effects are caused by the non-ferromagnetic properties.

In Refs. [10, 11] it was suggested that the small meV size activation energy of the resistivity could indicate a semiconductor. Such a small electronic gap can never remain open with an imperfect material as all these alloys are. Band bending and warping of the energy surfaces will close this small gap at some points in the Brillouin zone resulting at least in a zero gap material [28]. Such small gaps can only remain open when quantum mechanical effects prevail. These are meV gaps in superconductors (even amorphous and dirty Al is a superconductor) or hybridization gaps in intermediate valent or heavy fermion compounds [16]. In fact a gap due to correlated electron effects such as in a Kondo lattice has also been invoked in Refs. [10, 11]. However, in order that the carrier concentration exhibits a semiconducting behavior, the Fermi level must be in the gap, of whatever kind the gap is. The Luttinger theorem and its interpretation by Martin and Allen predict [15] (and it has been verified experimentally [16]) that the Fermi level can only be in a hybridization gap when the sum of f and d electrons is even.

In a trivalent Ce compound this sum is odd. So we do not expect a Kondo gap or hybridization gap with the Fermi level in the gap, and indeed this has been verified with the optical experiments. Instead, we proposed that the measured activation energy in the resistivity above T_C is due to a magnetic binding energy Δ, which is not governed by Fermi statistics. As a consequence one should write $\rho \propto \exp(\Delta/kT)$. There exist, however, several Ce^{3+} and Eu^{2+} compounds with odd f and d count with large gaps, e.g. Ce_2O_3 or EuO, which are paramagnetic insulators or ferromagnetic semiconductors, respectively.

Acknowledgment

The authors are grateful to Dr O. Vogt, Dr M. Filzmoser, and J. Malar for helpful discussions. They wish to thank P. Dekumbis, K. Mattenberger, J. Müller, and H.P. Staub for valuable technical assistance.

References

[1] O. Vogt, K. Mattenberger, in series *Handbook on the Physics, Chemistry of Rare Earths*, Eds. K.A. Gschneidner Jr., L. Eyring, G.H. Lander, G.R. Choppin, Vol. 17, Elsevier Science Publ., Amsterdam 1993, Ch. 114, 301.

[2] F. Salghetti-Drioli, K. Mattenberger, P. Wachter, L. Degiorgi, *Solid State Commun.*, in print.

[3] A. Schlegel, E. Kaldis, P. Wachter, Ch. Zürcher, *Phys. Lett. A* **66,** 125 (1978).

[4] F. Steglich, J. Aarts, C.D. Bredl, W. Lieke, D. Meschede, W. Franz, H. Schäfer, *Phys. Rev. Lett.* **43,** 1892 (1979).

[5] M.F. Hundley, P.C. Canfield, J.D. Thompson, Z. Fisk, *Phys. Rev. B* **42,** 6842 (1990).

[6] S.K. Malik, D.T. Adroia, *Phys. Rev. B* **43,** 6277 (1991).

[7] B. Bucher, Z. Schlesinger, P.C. Canfield, Z. Fisk, *Physica B* **199&200,** 489 (1994).

[8] T. Takabatake, G. Nakamoto, T. Yoshino, H. Fujii, K. Izawa, S. Nishigori, H. Goshima, T. Suzuki, T. Fujita, K. Maezawa, T. Hiraoka, Y. Okayama, I. Oguro, A.A. Menovsky, K. Neumaier, A. Brückl, K. Andres, *Physica B* **223&224,** 413 (1996).

[9] S.W. Tozer, A.W. Kleinsasser, T. Penney, D. Kaiser, F. Holzberg, *Phys. Rev. Lett.* **59**, 1768 (1987).

[10] S. Patil, Z. Hossain, P.L. Paulose, R. Nagarajan, L.C. Gupta, C. Godart, *Solid State Commun.* **99**, 419 (1996).

[11] P.L. Paulose, S. Patil, *J. Appl. Phys.* **81**, 5777 (1997).

[12] K. Fess, W. Kaefer, Ch. Thurner, K. Friemelt, Ch. Kloc, E. Bucher, *J. Appl. Phys.* **83**, 2568 (1998).

[13] P. Streit, P. Wachter, *Phys. kondens. Materie* **11**, 231 (1970).

[14] P. Wachter, in: *Alloys and Intermetallics*, Eds. K.A. Gschneidner Jr., L. Eyring, in series *Handbook on the Physics and Chemistry of Rare Earths*, Vol. 2, North-Holland, Amsterdam 1979, p. 507.

[15] R.M. Martin, J.W. Allen, *J. Appl. Phys.* **50**, 7561 (1979); L.M. Luttinger, *Phys. Rev.* **119**, 1153 (1960).

[16] P. Wachter, in: *Lanthanides/Actinides: Physics-II*, Eds. K.A. Gschneidner Jr., L. Eyring, G.H. Lander, G.R. Choppin, in series *Handbook on the Physics and Chemistry of Rare Earths*, Vol. 19, Elsevier Sciences B.V., Amsterdam 1994, p. 177.

[17] H. Langhof, *STADI-P*, STOE Application Laboratory, 1992.

[18] A.E. Dwight, *Acta Crystallogr. B* **33**, 1579 (1977).

[19] T. Herrmannsdörfer, P. Fischer, P. Wachter, G. Wetzel, K. Mattenberger, to be published.

[20] P. Wachter, *Phys. Lett. A* **58**, 484 (1976).

[21] S. von Molnar, F. Holtzberg, A. Benoit, A. Briggs, J. Flouquet, J.L. Toulance, in: *Valence Instabilities*, Eds. P. Wachter, H. Boppart, North-Holland, Amsterdam 1982, p. 579.

[22] M. Kasaya, K. Katoh, K. Takegahara, *Solid State Commun.* **78**, 797 (1991).

[23] R. Monnier, J. Rhyner, T.M. Rice, D.D. Koelling, *Phys. Rev. B* **31**, 5554 (1985).

[24] J. Allen, B. Batlogg, P. Wachter, *Phys. Rev. B* **20**, 4807 (1979).

[25] E.L. Nagaev, *JETP Lett.* **6**, 18 (1967).

[26] D. Kaczorowski, J. Schoenes, *Solid State Commun.* **74**, 143 (1990).

[27] P. Wachter, F. Bommeli, L. Degiorgi, P. Burlet, F. Bourdarot, E. Kaldis, *Solid State Commun.* **105**, 675 (1998).

[28] S. Broderick, V. Vescoli, B. Buschinger, W. Guth, O. Trovarelli, M. Weiden, L. Degiorgi, C. Geibel, F. Steglich, *Solid State Commun.* **108**, 463 (1998).

[29] L. Degiorgi, P. Wachter, D. Ihle, *Phys. Rev. B* **35**, 9259 (1987).